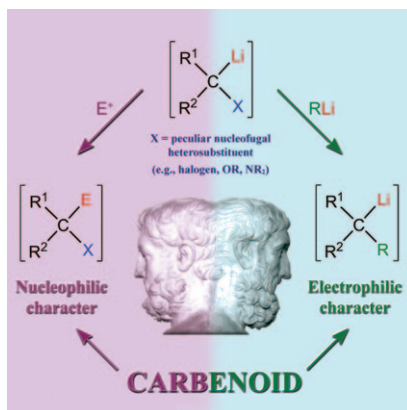


Face-to-face, rising to the challenge!

The two Janus-like souls of lithium carbenoids (see figure) are not a weak but, instead, a strong point of their reactivity. A proper knowledge of their structural features, aggregation, and solvation not only sheds light on the reasons for their thermal and configurational lability/stability, but can also allow a fine-tuning of their reactivity toward more stereoselective and targeted transformations.



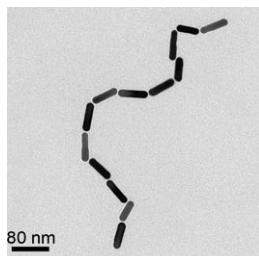
Lithium Carbenoids

V. Capriati,* S. Florio* 4152–4162

Anatomy of Long-Lasting Love Affairs with Lithium Carbenoids: Past and Present Status and Future Prospects

COMMUNICATIONS

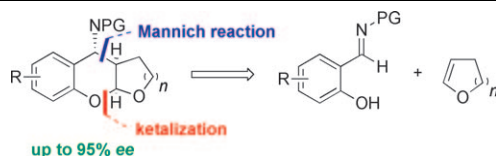
End-to-end connectivity of Au nanorods (NRs) employing bis(terpyridine)–metal (Fe^{II} or Cd^{II}) complexes has been demonstrated, along with their facile disassembly and reassembly. Biased surfactant adsorption at the side-walls allowed the predominant, end-facet modification of the NRs. Characterization included UV/Vis and X-ray photoelectron spectroscopy and TEM imaging.



Self-Assembly

Y.-T. Chan, S. Li, C. N. Moorefield, P. Wang, C. D. Shreiner, G. R. Newkome* 4164–4168

Self-Assembly, Disassembly, and Reassembly of Gold Nanorods Mediated by Bis(terpyridine)–Metal Connectivity



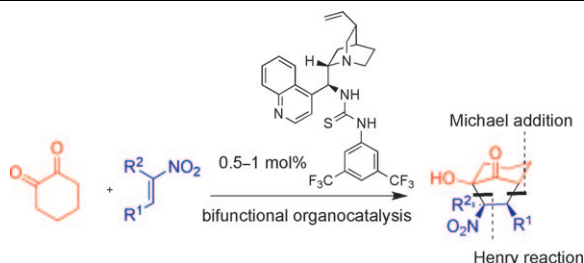
Domino catalysis: We have developed the first enantioselective domino Mannich–ketalization reaction of *o*-hydroxy benzaldimines with electron-rich alkenes (see scheme). The new reac-

tion sequence provides an easy and direct access to optically pure 4-aminobenzopyrans in good yields and with excellent enantiomeric ratios (up to e.r. 98:2).

Organocatalysis

M. Rueping,* M.-Y. Lin 4169–4172

Catalytic Asymmetric Mannich–Ketalization Reaction: Highly Enantioselective Synthesis of Aminobenzopyrans



Domino catalysis: Two consecutive quaternary stereocenters, three functional groups, and four stereogenic centers have been created in the newly

developed domino Michael–Henry reaction (see scheme) employing small amounts of a bifunctional organocatalyst.

Organocatalysis

M. Rueping,* A. Kuenkel, R. Fröhlich 4173–4176

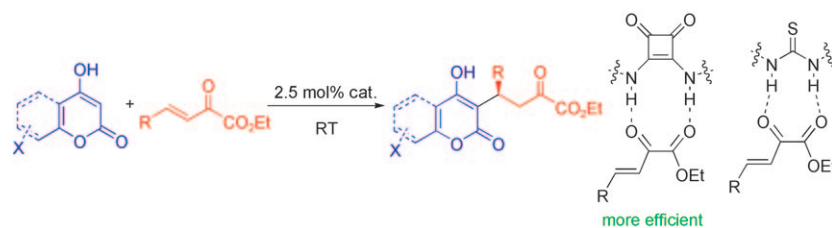
Catalytic Asymmetric Domino Michael–Henry Reaction: Enantioselective Access to Bicycles with Consecutive Quaternary Centers by Using Bifunctional Catalysts



Organocatalysis

D.-Q. Xu, Y.-F. Wang, W. Zhang,
S.-P. Luo, A.-G. Zhong, A.-B. Xia,
Z.-Y. Xu* 4177–4180

Chiral Squaramides as Highly Enantioselective Catalysts for Michael Addition Reactions of 4-Hydroxycoumarins and 4-Hydroxypyrene to β,γ -Unsaturated α -Keto Esters



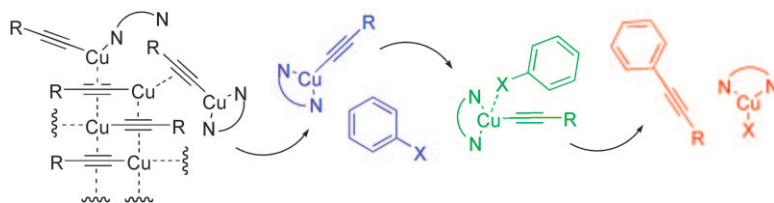
Distance brings forth beauty: The first highly enantioselective organocatalytic Michael addition of 4-hydroxycoumarins and the analogous 4-hydroxy-6-methyl-2-pyrene to β,γ -unsaturated

α -keto esters by using chiral squaramides as the organocatalysts is disclosed. The efficiency of the process is attributed to the hydrogen-bonding activation (see scheme).

Cross-Coupling Reactions

E. Zuidema, C. Bolm* 4181–4185

Sub-Mol % Catalyst Loading and Ligand-Acceleration in the Copper-Catalyzed Coupling of Aryl Iodides and Terminal Alkynes



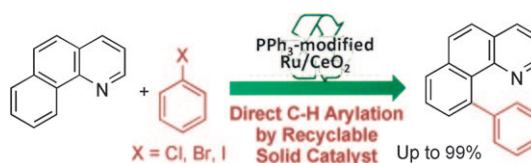
Just add ligand! The coupling of aryl iodides and terminal alkynes can be catalyzed with sub-mol % amounts of a copper complex. Addition of a large excess of diamine ligand converts the

inactive polymeric resting state of the catalyst into a highly active monomeric copper species, allowing the title reaction to be performed with such unprecedented low copper loadings.

Heterogeneous Catalysis

H. Miura, K. Wada,* S. Hosokawa,
M. Inoue 4186–4189

Recyclable Solid Ruthenium Catalysts for the Direct Arylation of Aromatic C–H Bonds



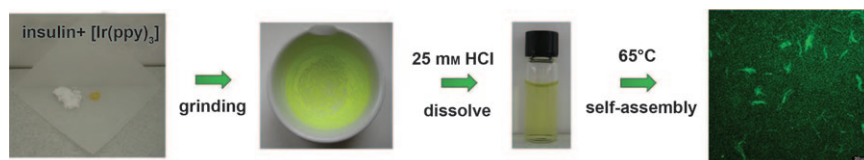
Environmentally benign catalyst: A PPh_3 -modified Ru/CeO_2 catalyst showed excellent catalytic activity toward direct C–H arylation by using various aryl chlorides in the reaction

(see scheme). The catalyst was found to act heterogeneously and could be recycled without significant loss of activity.

Self-Assembly

A. Rizzo, O. Inganäs,
N. Solin* 4190–4195

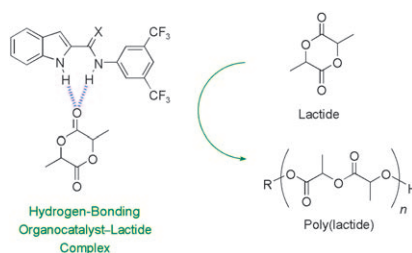
Preparation of Phosphorescent Amyloid-Like Protein Fibrils



Getting the green and red lights: A method to prepare amyloid-like fibrils functionalized with phosphorescent iridium complexes was developed. When heated in aqueous acid, the insulin–

iridium hybrid material self-assembles to form amyloid-like fibrils that emit light in the green or red range of the spectrum (see figure).

A fine blend of hydrogen bonds: New (thio)amidoindoles and (thio)amido-benzimidazoles catalyze the ring-opening polymerization of lactide in the presence of a cocatalyst (see scheme). A detailed investigation of weak interactions showed that these catalysts are still active despite two undesired pathways, self-aggregation, and hydrogen bonding between cocatalysts.



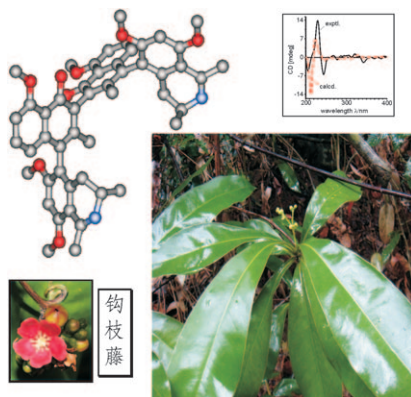
Ring-Opening Polymerization

S. Koeller, J. Kadota, F. Peruch, A. Deffieux, N. Pinaud, I. Pianet, S. Massip, J.-M. Léger, J.-P. Desvergne, B. Bibal* 4196–4205

(Thio)Amidoindoles and (Thio)Amido-benzimidazoles: An Investigation of Their Hydrogen-Bonding and Organocatalytic Properties in the Ring-Opening Polymerization of Lactide



Three consecutive chiral axes: Natural products with three chiral axes have been isolated from the Chinese plant *Ancistrocladus tectorius* (see picture) and their stereostructures characterized by spectroscopic and quantum chemical methods. These newly discovered dimeric naphthylisoquinoline alkaloids not only have intriguing chiral properties, but also promising anti-infective activities.



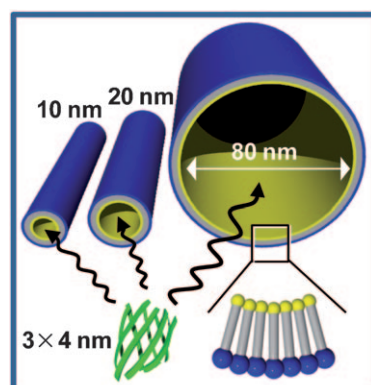
Natural Products

M. Xu, T. Bruhn, B. Hertlein, R. Brun, A. Stich, J. Wu, G. Bringmann* 4206–4216

Shuangancistrocladines A–E, Dimeric Naphthylisoquinoline Alkaloids with Three Chiral Biaryl Axes from the Chinese Plant *Ancistrocladus tectorius*



Inter-tubes: Diffusion constants and release rates of an encapsulated GFP in self-assembled organic nanotubes (see figure) decreased if the inner diameter of the nanochannels was decreased. Thermal and chemical stabilities of GFP in the nanochannels also strongly depended on the inner diameter size. The confinement effect allowed GFP to be stored stably at high temperatures and high denaturant concentrations.



Supramolecular Chemistry

N. Kameta,* H. Minamikawa, Y. Someya, H. Yui, M. Masuda, T. Shimizu* 4217–4223

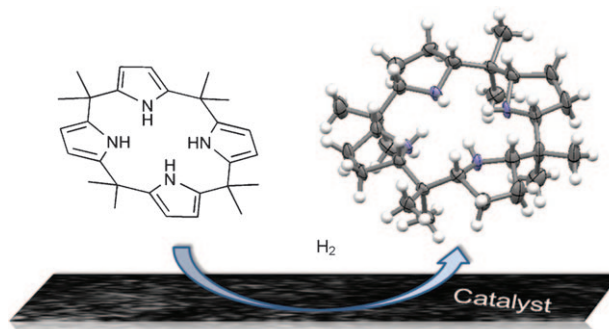
Confinement Effect of Organic Nanotubes Toward Green Fluorescent Protein (GFP) Depending on the Inner Diameter Size



Nitrogen Macrocycles

G. Journot, C. Letondor, R. Neier,*
H. Stoeckli-Evans, D. Savoia,
A. Gualandi* 4224–4230

Catalytic Hydrogenation of *meso*-Octamethylporphyrinogen (Calix[4]pyrrole)



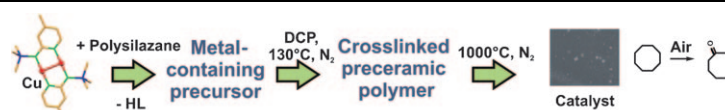
Calix[4]pyrrole reduction: Hydrogenation of calix[4]pyrrole with a number of heterogeneous catalysts under different experimental conditions has been investigated (see picture). The reaction proceeds with high diastereo-

selectivity to give only three diastereoisomers of the product derived from half-hydrogenation of the substrate, displaying alternating pyrrolidine and pyrrole rings, along with the all-*cis* saturated product.

Metal-Containing Ceramics

G. Glatz, T. Schmalz, T. Kraus,
F. Haarmann, G. Motz,*
R. Kempe* 4231–4238

Copper-Containing SiCN Precursor Ceramics (Cu@SiCN) as Selective Hydrocarbon Oxidation Catalysts Using Air as an Oxidant



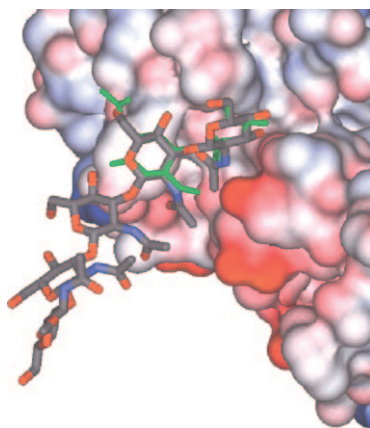
Choose the Cu content to suit: Copper aminopyridinates can react with polysilazane precursors by transmetalation. Crosslinking and ceramization of the metal-modified precursor lead to the copper-containing ceramic Cu@SiCN. Ceramics with a variable Cu content were synthesized and show catalytic

activity towards the oxidation of cycloalkanes by using air as oxidant. The selectivity can be tuned by varying the Cu content. These results confirm the potential of this new class of metal-containing ceramics as thermally robust and chemically highly inert catalysts.

Glycomimetics

M. Morando, Y. Yao,
S. Martín-Santamaría, Z. Zhu, T. Xu,
F. J. Cañada, Y. Zhang,*
J. Jiménez-Barbero* 4239–4249

Mimicking Chitin: Chemical Synthesis, Conformational Analysis, and Molecular Recognition of the $\beta(1\rightarrow3)$ N-Acetylchitopentose Analogue

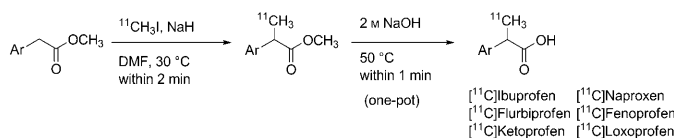


Chitin mimics in action: A synthetic chitin analogue, which is not hydrolyzed by a typical chitinase, still shows conformational and molecular recognition properties similar to those of the natural compound, as deduced from a combined NMR spectroscopic and modeling approach (see figure).

C–C Coupling

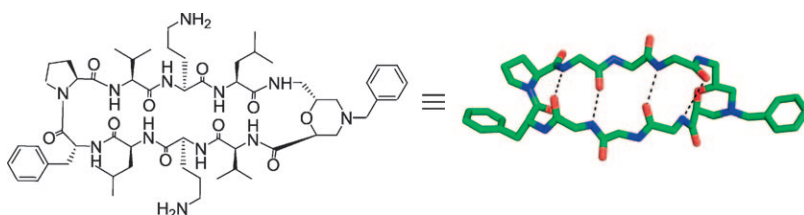
M. Takashima-Hirano, M. Shukuri,
T. Takashima, M. Goto, Y. Wada,
Y. Watanabe, H. Onoe, H. Doi,
M. Suzuki* 4250–4258

General Method for the ^{11}C -Labeling of 2-Arylpropionic Acids and Their Esters: Construction of a PET Tracer Library for a Study of Biological Events Involved in COXs Expression



Radiopharmaceuticals: To image cyclooxygenase-related pathological processes including inflammation, the ^{11}C -labeling method of 2-arylpropionic

acids (NSAIDs) was developed (see scheme). Their methyl esters were also prepared to increase the brain penetration.



Four analogues of the cyclic peptide antibiotic gramicidin S (GS) have been synthesized, in which the D-Phe-Pro dipeptide was replaced by a series of *cis*- and *trans*, δ - and ϵ -morpholine

amino acid (MAA). Interestingly, the derivative containing a *trans* δ -MAA is from a structural and functional point of view the best mimic of GS.

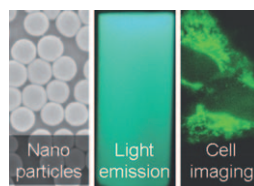
Peptidomimetics

V. V. Kapoerchan, E. Spalburg, A. J. de Neeling, R. H. Mars-Groenendijk, D. Noort, J. M. Otero, P. Ferraces-Casais, A. L. Llamas-Saiz, M. J. van Raaij, J. van Doorn, G. A. van der Marel, H. S. Overkleeft, M. Overhand* 4259–4265

Gramicidin S Derivatives Containing *cis*- and *trans*-Morpholine Amino Acids (MAAs) as Turn Mimetics



Highly emissive nanoparticles: Sol-gel reactions of tetraethyl orthosilicate (TEOS) and organic luminogens with aggregation-induced emission (AIE) characteristics furnish hybrid nanoparticles with core-shell structures in tunable sizes (45–295 nm). The nanoparticles are monodispersed and colloiddally stable. They emit strong visible light and function as selective cell-imaging bioprobes (see pictures).



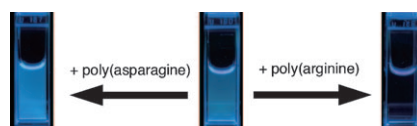
Nanoparticles

M. Faisal, Y. Hong, J. Liu, Y. Yu, J. W. Y. Lam, A. Qin, P. Lu, B. Z. Tang* 4266–4272

Fabrication of Fluorescent Silica Nanoparticles Hybridized with AIE Luminogens and Exploration of Their Applications as Nanobiosensors in Intracellular Imaging



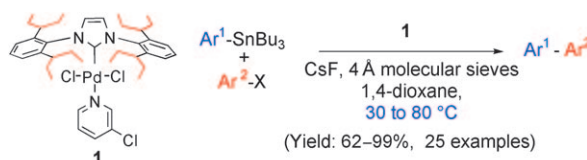
Lighten up: Apoferritin and its Tb^{3+} complex formed oligomeric and polymeric self-assemblies in neutral aqueous solutions. The apoferritin- Tb^{3+} complex assembly exhibited a particularly long-lived green luminescence in aqueous solution. This offered poly-(arginine)-selective precipitation, which was followed by monitoring the changes in luminescence. The poly-(arginine)-tagged albumin selectively and quantitatively precipitated with the apoferritin- Tb^{3+} complex.



Biosensors

H. Tsukube,* Y. Noda, S. Shinoda 4273–4278

Poly(arginine)-Selective Coprecipitation Properties of Self-Assembling Apoferritin and Its Tb^{3+} Complex: A New Luminescent Bioutil for Sensing of Poly(arginine) and Its Protein Conjugates



NHC-Pd (NHC = N-heterocyclic carbene) catalysts: Complex **1**, a highly hindered, but conformationally flexible catalyst, showed high efficiency in the Stille-Migita cross-coupling reaction of

challenging aryl halides and organostannanes. Complex **1** proved effective at temperatures as low as 30 °C; the current state-of-the-art method is heating in excess of 100 °C!

Cross-Coupling Reactions


M. Dowlut, D. Mallik, M. G. Organ* 4279–4283

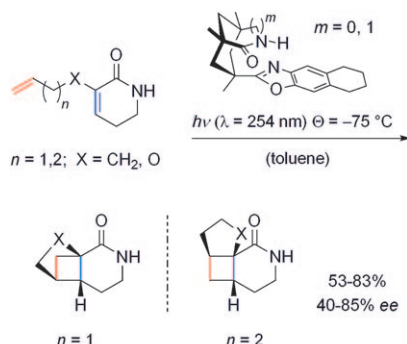
An Efficient Low-Temperature Stille-Migita Cross-Coupling Reaction for Heteroaromatic Compounds by Pd-PEPSSI-IPent



Asymmetric Synthesis

D. Albrecht, F. Vogt,
T. Bach* 4284–4296


 **Diastereo- and Enantioselective Intramolecular [2+2] Photocycloaddition Reactions of 3-(ω'-Alkenyl)- and 3-(ω'-Alkenyloxy)-Substituted 5,6-Dihydro-1H-pyridin-2-ones**

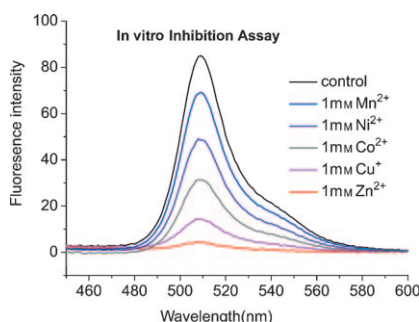


Template-induced enantioselectivities are achieved in the intramolecular [2+2] photocycloaddition reaction of 3-(ω'-alkenyl)- and 3-(ω'-alkenyloxy)-substituted 5,6-dihydro-1H-pyridin-2-ones, thus exclusively delivering the diastereomerically pure crossed ($n=1$) or straight ($n=2$) addition product depending on the chain length (see scheme). The noranalogue ($m=0$) of the established template ($m=1$) provided improved selectivity in three out of four cases.

Protein Splicing

L. Zhang, N. Xiao, Y. Pan, Y. Zheng,
Z. Pan, Z. Luo, X. Xu,
Y. Liu* 4297–4306

 **Binding and Inhibition of Copper Ions to RecA Inteins from *Mycobacterium tuberculosis***

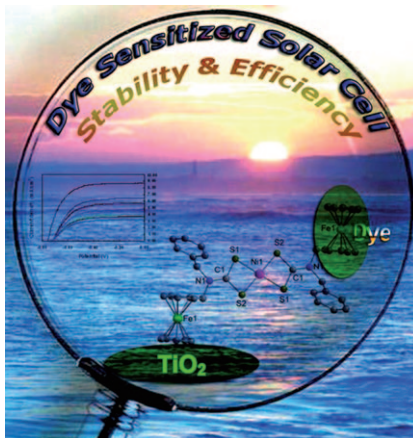


The dual role of copper: Both copper(II) and copper(I) bind to intein strongly, although at different key residues. Protein splicing can be inhibited by Cu^{II} due to strong coordination to the key residues (see graph). The slow oxidation of N-terminal cysteine and the binding of Cu^{I} also contribute to the inhibition properties.

Heterometallic Complexes

A. Kumar, R. Chauhan, K. C. Molloy,
G. Kociok-Köhn, L. Bahadur,*
N. Singh* 4307–4314

Synthesis, Structure and Light-Harvesting Properties of Some New Transition-Metal Dithiocarbamates Involving Ferrocene

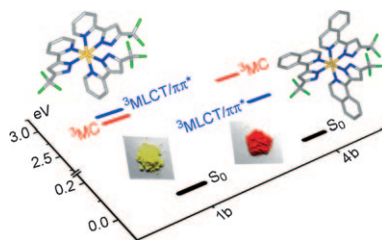


Making light work: Nine transition-metal dithiocarbamate complexes possessing ferrocenyl groups have been synthesised and their electrochemical and light-harvesting properties studied. The square-planar complexes containing Ni^{II} , Cu^{II} and Pt^{II} show the best performance for use in dye-sensitized solar cells (see picture).

Luminescence

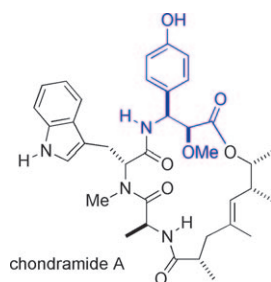
K. Chen, C.-H. Yang, Y. Chi,*
C.-S. Liu, C.-H. Chang, C.-C. Chen,
C.-C. Wu,* M.-W. Chung, Y.-M. Cheng,
G.-H. Lee, P.-T. Chou* 4315–4327

 **Homoleptic Tris(Pyridyl Pyrazolate) Ir^{III} Complexes: En Route to Highly Efficient Phosphorescent OLEDs**



Orange phosphorescence: Orange-emitting complex $\text{mer-}[\text{Ir}(\text{bipz})_3]$ was synthesized and shows the importance of lowering the $^3\text{MLCT}/\pi\pi^*$ energy level versus other high-lying excited states in designing highly efficient phosphors (see figure).

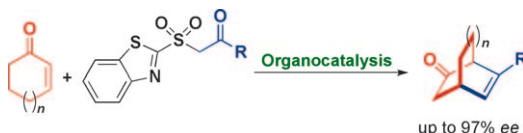
Stereochemistry clarified: Preparation of diastereomers of the β -amino- α -methoxy-propionic acid, contained in the cyclodepsipeptide chondramide A (see scheme), allowed for the determination of the stereochemistry of this part. The correct 2,3-*anti*-diastereomer was obtained by an asymmetric dihydroxylation reaction followed by a regioselective Mitsunobu reaction with hydrazoic acid. A Mitsunobu reaction was also used for formation of the ester bond of chondramide A.



Natural Products

A. Schmauder, L. D. Sibley,
M. E. Maier* 4328–4336

Total Synthesis and Configurational Assignment of Chondramide A



Bicycle race: A facile organocatalytic route to optically active 6-substituted bicyclo[2.2.2]oct-5-en-2-ones is presented. The key step is the enantioselective 1,4-addition of β -keto benzothiazoylsulfones to α,β -unsaturated

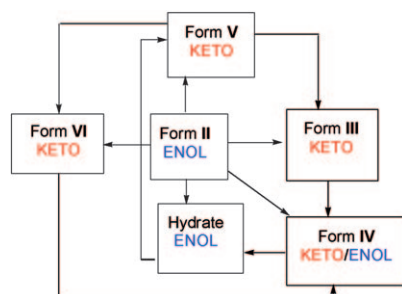
cyclic ketones. Subsequent intramolecular aldol reaction and Smiles rearrangement gives rise to the optically active bicyclic compounds (see scheme).

Asymmetric Organocatalysis

N. Holub, H. Jiang, M. W. Paixão,
C. Tiberi, K. A. Jørgensen* 4337–4346

An Unexpected Michael–Aldol–Smiles Rearrangement Sequence for the Synthesis of Versatile Optically Active Bicyclic Structures by Using Asymmetric Organocatalysis

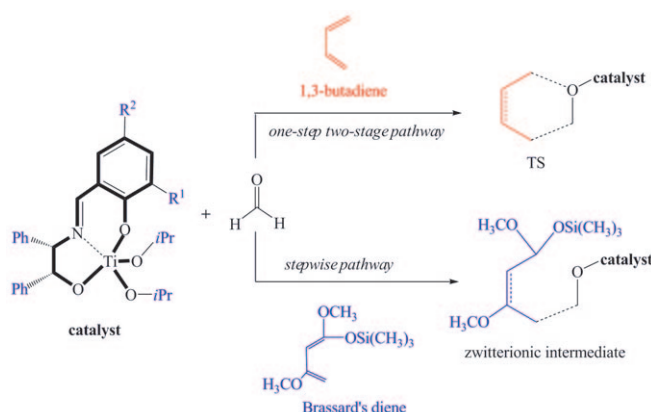
Shifting states: The richest collection of tautomeric polymorphic forms so far reported in the literature has been studied (see figure). Five new polymorphs and one hydrated form of 2-thiobarbituric acid have been isolated and characterised by solid-state methods as keto, enol or hybrid isomers. Mechanical methods have induced keto–enol conversions between the forms.



Polymorphism

M. R. Chierotti,* L. Ferrero, N. Garino,
R. Gobetto, L. Pellegrino, D. Braga,
F. Grepioni, L. Maini* 4347–4358

The Richest Collection of Tautomeric Polymorphs: The Case of 2-Thiobarbituric Acid



Different pathways are followed in hetero-Diels–Alder reactions of Brassard's diene and butadiene catalyzed by a titanium(IV) complex of a tridentate Schiff base according to mechanistic investigations by DFT and ONIOM

methods. The OCH_3 and $\text{OSi}(\text{CH}_3)_3$ substituents of Brassard's diene play the key role in the formation of the transition state and zwitterionic intermediate (see scheme) by participating in charge transfer to formaldehyde.

Reaction Mechanisms

Z. Su, S. Qin, C. Hu,*
X. Feng* 4359–4367

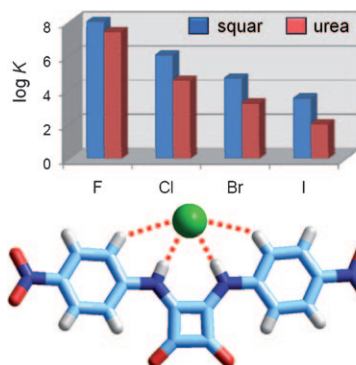
Theoretical Investigations on the Mechanism of Hetero-Diels–Alder Reactions of Brassard's Diene and 1,3-Butadiene Catalyzed by a Tridentate Schiff Base Titanium(IV) Complex



Anion Recognition

V. Amendola, G. Bergamaschi,
M. Boiocchi, L. Fabbrizzi,*
M. Milani 4368–4380

The Squaramide versus Urea Contest for Anion Recognition

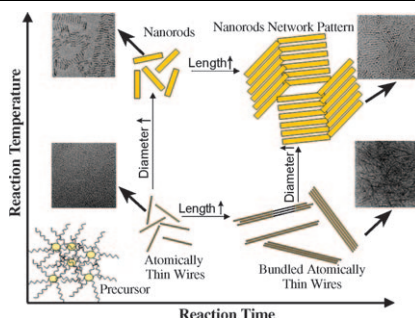


A four hydrogen-bond donor: A squaramide-based receptor forms 1:1 complexes with halide ions 1 to 2 orders of magnitude more stable than the corresponding renowned urea-based receptor, as it is able to donate to the anion two hydrogen bonds from C_α–H fragments in addition to the two hydrogen bonds from amide N–H groups, thus making a total of four (see image).

Anatase Wires

C. Liu, H. Sun, S. Yang*... 4381–4393

From Nanorods to Atomically Thin Wires of Anatase TiO₂: Nonhydrolytic Synthesis and Characterization

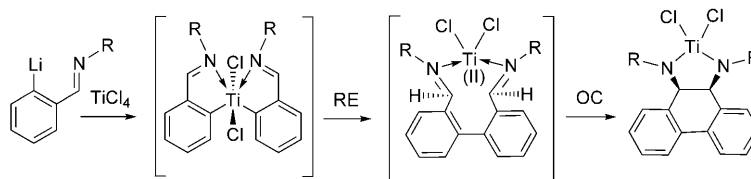


The ultimate slimming process? A two-step method has been developed to produce ultrathin titania wires with tunable diameters ranging from the nm to the Å scale as shown. Spectroscopic characterization has uncovered dramatic size effects on the vibrational and electronic structures of the titania wires in the smallest size regime that open up new possibilities of tailoring material properties for nano- to atomic-scale devices.

Domino Reactions

D. Zhao, W. Gao, Y. Mu,*
L. Ye 4394–4401

Direct Synthesis of Titanium Complexes with Chelating *cis*-9,10-Dihydrophenanthrenediamide Ligands through Sequential C–C Bond-Forming Reactions from *o*-Metalated Arylimines



In situ formation of ligand: Ti^{IV} complexes with *cis*-9,10-dihydrophenanthrenediamide ligands were synthesised directly from TiCl₄ and the corresponding *o*-C₆H₄(CH=NR)Li through

a novel intramolecular C–C bond-forming sequence of reductive elimination (RE) and oxidative coupling (OC; see scheme).

* Author to whom correspondence should be addressed

VIP Full Papers labeled with this symbol have been judged by two referees as being “very important papers”.

Supporting information on the WWW (see article for access details).

Video A video clip is available as Supporting Information on the WWW (see article for access details).

SERVICE

Spotlights 4148 Author Index 4402 Keyword Index 4403 Preview 4405

Issue 13/2010 was published online on March 26, 2010